

Superconductivity and Madelung potential of $\text{YBa}_2\text{Cu}_3\text{O}_{6+x}$ ordered superstructures

Qiang Wang

Department of Physics, Peking University, Beijing 100871, People's Republic of China

Han Rushan, D. L. Yin, and Z. Z. Gan

China Center of Advanced Science and Technology (World Laboratory), P.O. Box 8730, Beijing, People's Republic of China

(Received 30 October 1991; revised manuscript received 2 March 1992)

The Madelung potential of each possible ordered superlattice of $\text{YBa}_2\text{Cu}_3\text{O}_{6+x}$ is calculated as the oxygen content x varies from zero to 1. ΔV_A , the difference in Madelung site potential between apex and in-plane (CuO_2) oxygen atoms, is presented as a function of the composition x . The correlation of T_c and x is discussed in terms of Ohta's empirical curve of T_c vs ΔV_A . The theoretical results suggest that the superconductivity depends on the superlattice structure.

The physical properties, resistivity, magnetic susceptibility, and the temperatures of the structural phase transition and of the superconducting transition of the high- T_c oxide superconductors are quite sensitive to oxygen stoichiometry, and specifically to the positions of the oxygen atoms.^{1,2} In $\text{YBa}_2\text{Cu}_3\text{O}_{6+x}$, T_c depends on x . Figure 1 shows the change of T_c with the oxygen content. On the other hand, corresponding structures that differ in the arrangement of oxygen atoms in the CuO_x planes have been reported to exist for different values of x at low temperatures.³ The reported superstructures were the tetragonal phase for $x=0$, the orthorhombic phase for $x=1$,⁴ and the orthorhombic with a double unit cell for $x=\frac{1}{2}$.^{5,6} More complex superstructures were observed for $x=\frac{7}{8}$,^{7,8} x near $\frac{3}{5}$,⁹ and x near $\frac{2}{3}$.¹⁰ A recently observed structure is the tetragonal phase for $x=\frac{3}{8}$.¹¹ For $x=\frac{1}{4}$ and $\frac{3}{4}$, a set of superstructures have been proposed.¹² To establish a relationship between the various observed types of oxygen ordering in the Cu-O basal plane and their superconductivities, a variable ΔV_A defined

within an ionic model¹³ is used. ΔV_A equals the difference between $V_{O(A)}$ and $V_{O(P)}$, where V_i [$i=O(A), O(P)$] is the Madelung site potential for a given charge distribution of corresponding superstructure. $O(A)$ and $O(P)$ denote the apex and in-plane (CuO_2) oxygen atoms, respectively.

Several experimentally observed and theoretically possible superstructures at low temperature in $\text{YBa}_2\text{Cu}_3\text{O}_{6+x}$ systems with different x are shown in Fig. 2, where the distributions of oxygen atoms and oxygen vacancies in the Cu-O basal plane is exhibited. The valence of Cu in the plane is assigned in terms of the following rules:¹⁴

O-Cu-O, fourfold coordination Cu with a valence of +2,

□-Cu-□, twofold coordination Cu with a valence of +1,

O-Cu-□, threefold coordination Cu with a valence of +2.

Therefore, the valence of all ions of each superstructure in the $\text{YBa}_2\text{Cu}_3\text{O}_{6+x}$ system is given for different x with the condition of compound charge neutrality (see Fig. 2):

- (1) $\text{YBa}_2\text{Cu}_3\text{O}_7$ $\text{Y}^{3+} + 2\text{Ba}^{2+} + \text{O}^{2-} + 2\text{Cu}^{2+} + \text{O}^{1.75-} + \text{Cu}^{2+} + \text{O}^{2-}$
- (2) $\text{YBa}_2\text{Cu}_3\text{O}_{6.875}$ (a) $8\text{Y}^{3+} + 16\text{Ba}^{2+} + \text{O}^{2-} + 16\text{Cu}^{2+} + \text{O}^{1.78125-} + 7\text{Cu}^{2+} + \text{Cu}^{1+} + 7\text{O}^{2-}$
(b) $8\text{Y}^{3+} + 16\text{Ba}^{2+} + \text{O}^{2-} + 16\text{Cu}^{2+} + \text{O}^{1.75-} + 6\text{Cu}^{2+} + 2\text{Cu}^{1+} + 7\text{O}^{2-}$
- (3) $\text{YBa}_2\text{Cu}_3\text{O}_{6.75}$ (a) $4\text{Y}^{3+} + 8\text{Ba}^{2+} + \text{O}^{2-} + 8\text{Cu}^{2+} + \text{O}^{1.8125-} + 3\text{Cu}^{2+} + \text{Cu}^{1+} + 3\text{O}^{2-}$
(b) $4\text{Y}^{3+} + 8\text{Ba}^{2+} + \text{O}^{2-} + 8\text{Cu}^{2+} + \text{O}^{1.875-} + 4\text{Cu}^{2+} + 3\text{O}^{2-}$
- (4) $\text{YBa}_2\text{Cu}_3\text{O}_{6.67}$ $3\text{Y}^{3+} + 6\text{Ba}^{2+} + \text{O}^{2-} + 6\text{Cu}^{2+} + \text{O}^{1.83334-} + 2\text{Cu}^{2+} + \text{Cu}^{1+} + 2\text{O}^{2-}$
- (5) $\text{YBa}_2\text{Cu}_3\text{O}_{6.6}$ $5\text{Y}^{3+} + 10\text{Ba}^{2+} + \text{O}^{2-} + 10\text{Cu}^{2+} + \text{O}^{1.85-} + 3\text{Cu}^{2+} + 2\text{Cu}^{1+} + 3\text{O}^{2-}$
- (6) $\text{YBa}_2\text{Cu}_3\text{O}_{6.5}$ $2\text{Y}^{3+} + 4\text{Ba}^{2+} + \text{O}^{2-} + 4\text{Cu}^{2+} + \text{O}^{1.875-} + \text{Cu}^{2+} + \text{Cu}^{1+} + \text{O}^{2-}$
- (7) $\text{YBa}_2\text{Cu}_3\text{O}_{6.375}$ (a) $8\text{Y}^{3+} + 16\text{Ba}^{2+} + \text{O}^{2-} + 16\text{Cu}^{2+} + \text{O}^{1.90625-} + 3\text{Cu}^{2+} + 5\text{Cu}^{1+} + 3\text{O}^{2-}$
(b) $8\text{Y}^{3+} + 16\text{Ba}^{2+} + \text{O}^{2-} + 16\text{Cu}^{2+} + \text{O}^{2-} + 6\text{Cu}^{2+} + 2\text{Cu}^{1+} + 3\text{O}^{2-}$
- (8) $\text{YBa}_2\text{Cu}_3\text{O}_{6.25}$ (a) $4\text{Y}^{3+} + 8\text{Ba}^{2+} + \text{O}^{2-} + 8\text{Cu}^{2+} + \text{O}^{1.9375-} + 3\text{Cu}^{2+} + \text{Cu}^{1+} + \text{O}^{2-}$
(b) $4\text{Y}^{3+} + 8\text{Ba}^{2+} + \text{O}^{2-} + 8\text{Cu}^{2+} + \text{O}^{2-} + 2\text{Cu}^{2+} + 2\text{Cu}^{1+} + \text{O}^{2-}$
- (9) $\text{YBa}_2\text{Cu}_3\text{O}_6$ $\text{Y}^{3+} + 2\text{Ba}^{2+} + \text{O}^{2-} + 2\text{Cu}^{2+} + \text{O}^{2-} + \text{Cu}^{2+}$

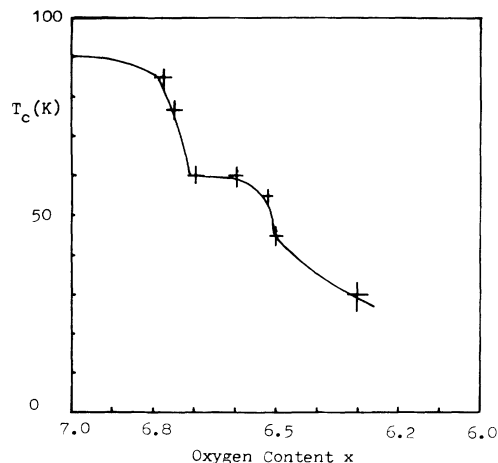


FIG. 1. Correlation of superconducting transition temperature T_c and composition x in $YBa_2Cu_3O_{6+x}$, derived from Ref. 1.

The structural type and hole densities are listed in Table I.

We assume the charge on each ion is distributed as a point charge, i.e., ionic model. Such an ionic approximation has been shown¹⁵ to be complementary to normal band-structure calculations. More accurate calculations will improve and go beyond this model, but the essential physics will remain.¹⁶ Because the compounds under study are ionic crystals and the most important factors to determine the hole distribution are the Madelung energy, the ionization energy of cations, and the electron affinity of anions, the ionic model is appropriate for calculating the site potential of this compound, although covalency may also play an important role in some cases.¹⁷ For each superstructure and corresponding valence distribution the Madelung potentials of each ion in the unit cell are calculated by use of the standard Ewald method. The Madelung potentials are listed in Table II. For the case when all the ordered states of $YBa_2Cu_3O_{6+x}$ ($0 < x < 1$) are the orthorhombic superstructures, the curve of ΔV_A versus concentration x is sketched in Fig. 3. Using Ohta's empirical curve¹³ showing $T_c = 0$ when $\Delta V_A < -2$ (eV), the curve of T_c vs x is obtained and shown in Fig. 4. As a result, it is predicted that the Y system is superconducting for the whole range of $0 < x < 1$. For the case when the ordered states of $YBa_2Cu_3O_{6.75}$, $YBa_2Cu_3O_{6.375}$, and $YBa_2Cu_3O_{6.25}$ are taken as tetragonal superstructures, and the others as still orthorhombic, the curve of ΔV_A vs x in Fig. 5 is obtained. The function of T_c vs x that results is shown in Fig. 6 by use of the same empirical curve of T_c vs ΔV_A .¹³ From Fig. 6 it is clear that T_c decreases as x decreases and finally approaches zero at about $x = 0.4$, while the corresponding hole density in the plane is zero

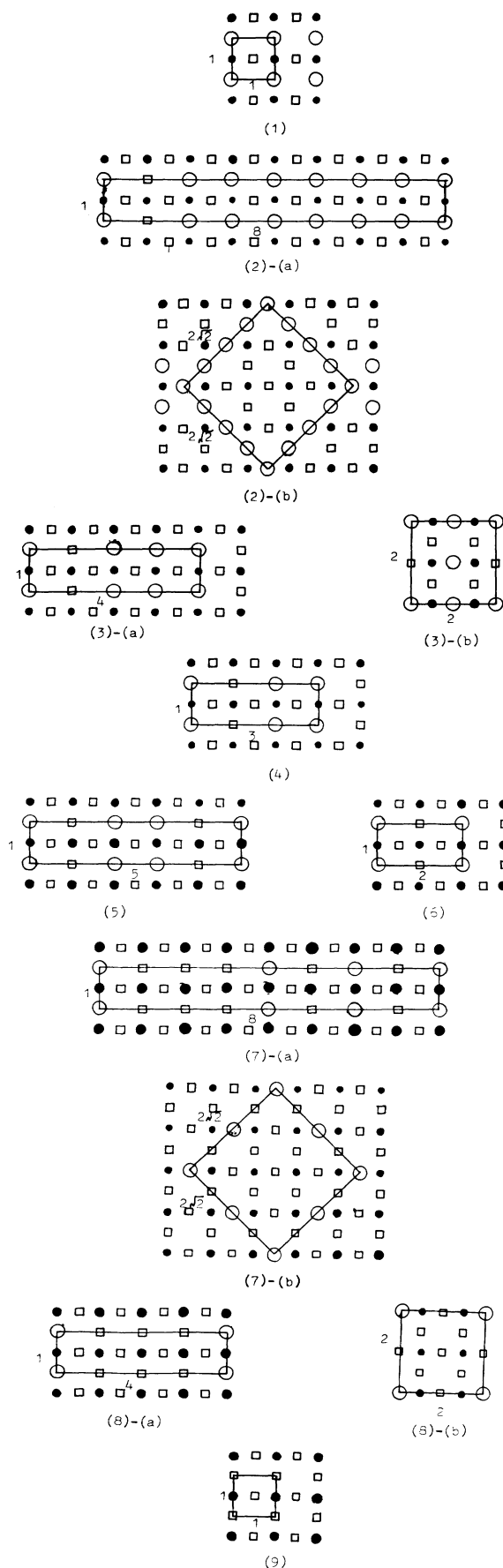


FIG. 2. Several possible superstructures at low temperature in the $YBa_2Cu_3O_{6+x}$ system: ●, copper; ○, oxygen; □, oxygen vacancy; the lines show the superstructural unit cell. (1) $YBa_2Cu_3O_7$; (2) $YBa_2Cu_3O_{6.875}$; (3) $YBa_2Cu_3O_{6.75}$; (4) $YBa_2Cu_3O_{6.67}$; (5) $YBa_2Cu_3O_{6.6}$; (6) $YBa_2Cu_3O_{6.5}$; (7) $YBa_2Cu_3O_{6.375}$; (8) $YBa_2Cu_3O_{6.25}$; (9) $YBa_2Cu_3O_6$.

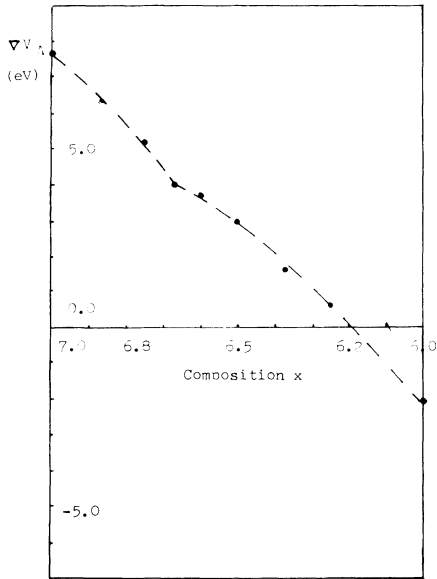


FIG. 3. Curve of ΔV_A vs concentration x when all ordered states are orthorhombic.

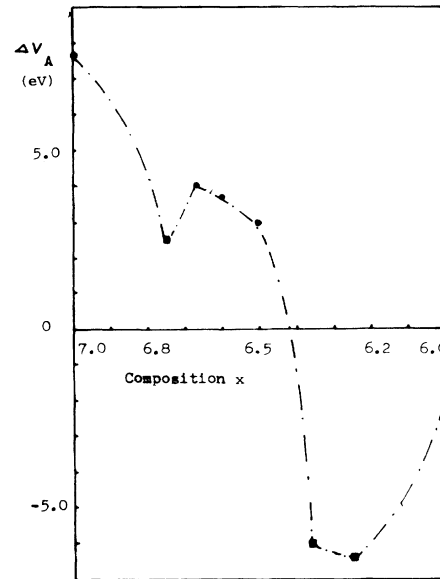


FIG. 5. Curve of ΔV_A vs concentration x when part of the superstructures are tetragonal and others are still orthorhombic.

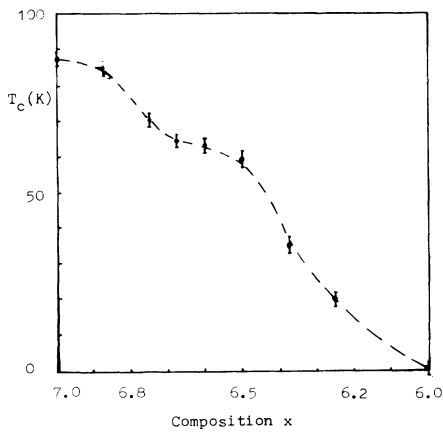


FIG. 4. Curve of T_c vs concentration x for all orthorhombic states.

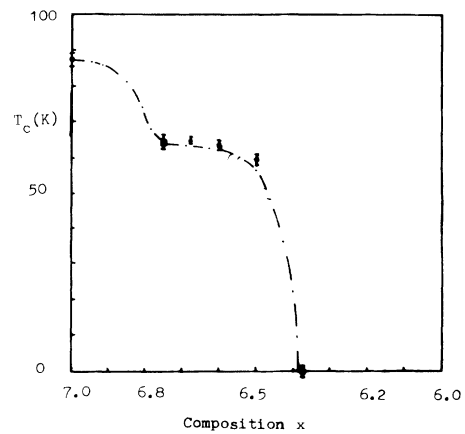


FIG. 6. Curve of T_c vs concentration x for the second case.

TABLE I. Superstructure type and carrier density in $YBa_2Cu_3O_{6+x}$ systems.

Compound	Superstructure type	Hole density in CuO_2	Electron density in basal plane
$YBa_2Cu_3O_7$	1×1 orthorhombic	1.0	0.0
$YBa_2Cu_3O_{6.875}$	(a) 8×1 orthorhombic	0.875	0.125
	(b) $2\sqrt{2} \times 2\sqrt{2}$ tetragonal	1.0	0.25
$YBa_2Cu_3O_{6.75}$	(a) 4×1 orthorhombic	0.75	0.25
	(b) 2×2 tetragonal	0.5	0.0
$YBa_2Cu_3O_{6.67}$	3×1 orthorhombic	0.67	0.33
$YBa_2Cu_3O_{6.6}$	5×1 orthorhombic	0.6	0.4
$YBa_2Cu_3O_{6.5}$	2×1 orthorhombic	0.5	0.5
$YBa_2Cu_3O_{6.375}$	(a) 8×1 orthorhombic	0.375	0.625
	(b) $2\sqrt{2} \times 2\sqrt{2}$ tetragonal	0	0.25
$YBa_2Cu_3O_{6.25}$	(a) 4×1 orthorhombic	0.25	0.75
	(b) 2×2 tetragonal	0	0.5
$YBa_2Cu_3O_6$	1×1 tetragonal	0	1.0

TABLE II. Madelung potentials of apex and in-plane oxygen atoms.

Compounds	Structural type	$V_{O(A)}$ ^a (a.u.)	$V_{O(P)}$ ^a (a.u.)	$\Delta V_A = V_{O(A)} - V_{O(P)}$ ^a (eV)
YBa ₂ Cu ₃ O ₇	Orthorhombic	-0.612	-0.897	7.70
YBa ₂ Cu ₃ O _{6.875}	Orthorhombic	-0.630	-0.872	6.28
	Tetragonal	-0.476 ^b	-0.883	· · ·
YBa ₂ Cu ₃ O _{6.75}	Orthorhombic	-0.658	-0.850	5.18
	Tetragonal	-0.712	-0.802	2.43
YBa ₂ Cu ₃ O _{6.67}	Orthorhombic	-0.687	-0.834	3.94
YBa ₂ Cu ₃ O _{6.6}	Orthorhombic	-0.683	-0.818	3.65
YBa ₂ Cu ₃ O _{6.5}	Orthorhombic	-0.694	-0.801	2.91
YBa ₂ Cu ₃ O _{6.375}	Orthorhombic	-0.720	-0.780	1.62
	Tetragonal	-0.762	-0.535	-6.13
YBa ₂ Cu ₃ O _{6.25}	Orthorhombic	-0.728	-0.753	0.68
	Tetragonal	-0.974	-0.735	-6.45
YBa ₂ Cu ₃ O ₆	Tetragonal	-0.775	-0.706	-1.86

^aAverage value over different sites in the superstructural unit cell.

^bThis value is more than -0.5 (a.u.), the critical value of the Madelung potential for a stable O²⁻ ion, leading to unstable structure. Therefore, the corresponding ΔV_A is excluded in this model.

but the in-plane electron density is not zero as given in the Table I. This is consistent with YBa₂Cu₃O_{6+x} being a hole-type superconductor. Comparing Figs. 4 and 6, we can conclude that the theoretical prediction in Fig. 6 is in much better agreement with the experimental results¹ in Fig. 1. It is further concluded that the structures of YBa₂Cu₃O_{6.375} and YBa₂Cu₃O_{6.25} systems are tetragonal and those systems have valence distributions that lead to zero hole density in the CuO₂ planes.

Ohta, Tohyama, and Maekawa¹³ thought that the energy splitting ΔE_z between the in-plane (CuO₂) and out-of-plane $2p$ - $3d$ transition correlates with T_c , in particular, with the one-body energy level splittings $\Delta \epsilon_A$ [for the P_z orbital of O(A) relative to P_σ orbital of O(P)] and $\Delta \epsilon_d$ (for the $3z^2-r^2$ orbital of Cu $3d$ relative to its x^2-y^2 orbital). Madelung potentials are screened due to core polarization to give, e.g., the energy levels $\Delta \epsilon_A = \Delta V_A / \epsilon(\infty)$, where $\epsilon(\infty)$ is the dielectric constant at optical frequen-

cies. Crystal-field theory suggests that $\Delta \epsilon_d$ may be linked with ΔV_A . Thus, a larger ΔV_A yields a larger $\Delta \epsilon_A$ and $\Delta \epsilon_d$, leading to the larger ΔE_z . Covalency between the P_z and $3z^2-r^2$ orbitals may be suppressed due to the splitting $\Delta \epsilon_A$, which also enhances ΔE_z . It seems clear that there is a strong correlation between the ΔV_A and the superconducting temperature; in other words, any parameters or factors changing ΔV_A will influence T_c . We have shown that the relationship between T_c and concentration x in the YBa₂Cu₃O_{6+x} system can be interpreted by using an empirical curve of ΔV_A and T_c . Recently, Ledbetter and Lei¹⁸ presented a direct relationship between ΔV_A and T_c . This, of course, suggests that the relation of ΔV_A and T_c is worth studying further theoretically and experimentally.

This work was supported by the National Postdoctoral Grant of China.

¹R. J. Cava, B. Batlogg, C. H. Chen, E. A. Rietman, S. M. Zahurak, and D. Werder, Phys. Rev. B **36**, 5719 (1987).

²Z. Z. Wang, J. Clayhold, N. P. Ong, J. M. Tarascon, L. H. Greene, W. R. McKinnon, and G. W. Hull, Phys. Rev. B **36**, 7222 (1987).

³A. A. Aligia, H. Bonadeo, and J. Garces, Phys. Rev. B **43**, 542 (1991).

⁴J. D. Jorgensen, M. A. Beno, D. G. Hinks, L. Soderholm, K. J. Volin, R. L. Hitterman, J. D. Grace, I. K. Schuller, C. U. Segre, K. Zhang, and M. S. Kleefisch, Phys. Rev. B **36**, 3608 (1987).

⁵G. Van Tendeloo, H. W. Zandbergen, and S. Amelinckx, Solid State Commun. **63**, 603 (1987).

⁶C. Chaillout, M. A. Alario-Franco, J. J. Capponi, J. Chenavas, P. Strobel, and M. Marezio, Solid State Commun. **65**, 283 (1988).

⁷M. A. Alario-Franco, C. Chaillout, J. J. Capponi, J. Chenavas, and M. Marezio, Physica C **156**, 455 (1988).

⁸J. L. Hodeau, P. Bordet, J. J. Capponi, C. Chaillout, and M. Marezio, Physica C **153-155**, 582 (1988).

⁹D. J. Werder, C. H. Chen, R. J. Cava, and B. Batlogg, Phys. Rev. B **37**, 2317 (1988).

¹⁰D. J. Werder, C. H. Chen, R. J. Cava, and B. Batlogg, Phys. Rev. B **38**, 5130 (1988).

¹¹R. Sonntag, D. Hohlwein, T. Bruckel, and G. Collin, Phys. Rev. Lett. **66**, 1497 (1991).

¹²J. Reyes-Gasga, T. Krekels, G. Van Tendeloo, J. Van Landuyt, S. Amelinckx, W. H. M. Bruggink, and H. Verweij, Physica C **159**, 831 (1989).

¹³Y. Ohta, T. Tohyama, and S. Maekawa, Physica B **165 & 166**, 983 (1990).

¹⁴Han Rushan, Gan Zizhao, Yin Daole, and Liao Qing, Phys. Rev. B **41**, 6683 (1990).

¹⁵R. E. Cohen, W. E. Pickett, H. Krakauer, and L. L. Boyer, Physica B **150**, 61 (1988).

¹⁶J. B. Torrance and R. M. Metzger, Phys. Rev. Lett. **63**, 1515 (1989).

¹⁷J. Kondo, Y. Asai, and S. Naga, J. Phys. Soc. Jpn. **57**, 4343 (1988).

¹⁸H. Ledbetter and Ming Lei, Physica C **177**, 86 (1991).